



I S A V

**Journal of Theoretical and Applied
Vibration and Acoustics**

journal homepage: <http://tava.isav.ir>



Free vibration analysis of variable stiffness composite laminated thin skew plates using IGA

Vahid Khalafi^a, Jamshid Fazilati^{b*}

^a Ph.D. student, Aerospace research institute, Mahestan St., Tehran, Iran

^b Faculty member, Aerospace research institute, Mahestan St., Tehran, Iran

ARTICLE INFO

Article history:

Received 26 February 2018

Received in revised form
23 December 2018

Accepted 25 December 2018

Available online 28 December
2018

Keywords:

Isogeometric analysis,

Curvilinear fibers laminate,

Skew plate,

Free vibration.

ABSTRACT

A NURBS-based isogeometric finite element formulation is developed and adopted to the free vibration analysis of finite square and skew laminated plates. Variable stiffness plies are assumed due to implementation of curvilinear fiber reinforcements. It is assumed due to employment of tow placement technology, in each ply of variable stiffness composite laminated plate the fiber reinforcement orientation angle is changed linearly with respect to longitudinal geometry coordinate. The classic plate theory is utilized for structural model description. The cubic NURBS basis functions are employed to approximate the geometry of the plate while simultaneously serve as the shape functions for solution field approximation in the analysis. To show the effectiveness and accuracy of the developed formulation, some representative results are extracted and compared to similar items available in the literature. The effects of curvilinear fiber angles, different geometries and various end constraints are evaluated on the variable stiffness composite laminated skew panel behavior.

© 2018 Iranian Society of Acoustics and Vibration, All rights reserved.

1. Introduction

The isogeometric analysis (IGA) that was firstly proposed by Hughes *et al.*[1]. aimed to unify the processes within geometrical computer aided design (CAD) and the finite element (FEM) model. The main sense of the IGA is to implement the base functions of CAD approximations (e.g., the NURBS) into elemental shape functions of the FEM in approximating the field

*Corresponding author:

E-mail address: jfazilati@ari.ac.ir (J. Fazilati)

<http://dx.doi.org/10.22064/tava.2018.81281.1100>

variables while at the same time describe the geometry of engineering components used in analytical process.

Preserving the exact geometry at the coarsest discretization level and performing of re-meshing process at this level without any further communication with CAD geometry are among the great advantageous features of the IGA formulation. These achievements could be gained while utilizing the B-spline, NURBS or T-spline functions in both CAD geometry outfitting and in representation of the FEM unknown approximation fields. The NURBS basis functions especially is noticeable in meeting the expected requirements. The use of IGA formulation is nowadays outspread to various mechanics and physics fields of study among them fluid-structure interaction and structural analysis [2-4]. The free vibration behavior of variable stiffness composite laminates (VSCL) skew plates with curvilinear fiber reinforcements by using the isogeometric finite element method associated with the NURBS shape functions is the main subject of the present paper. In terms of the finite element methodology based on the Kirchhoff theory, at least C^1 inter-elemental continuity is mandatory. Many complexities may emerge in case of the free-form geometries and boundaries while using the standard Lagrangian polynomials as FEM basis functions. The high order NURBS basis functions (functions of order 3 and higher) could be easily obtained with an increased inter-elemental continuity. Thus the NURBS function is well suited for the Kirchhoff elements through the IGA formulation. Shojaee *et al.*[5] performed isogeometric finite element analysis of free vibration of isotropic thin plates based on the classical plate theory. Non-Uniform Rational B-Splines (NURBS) basis functions were utilized as the approximating functions of the thin plate displacement field while are also describing the exact geometry. Several numerical simulations of thin plates with various shapes including square, circular, skew, and L-shape plate with complicated cutouts were examined. It was shown that the developed formulation is able to yield highly accurate predictions. They [6] also utilized the classical isogeometric finite element method in order to investigate the natural frequencies and buckling behavior of laminated plates. Lagrange multiplier method besides an orthogonal transformation technique were applied to meet the essential boundary conditions. Some numerical problems of laminated plates with different boundary conditions, fiber orientations, and lay-ups were also presented. The static deflection and the free vibration behavior of curvilinear stiffened plates was investigated by Qin *et al.*[7]. NURBS based isogeometric approach was utilized. The large deformation and the large amplitude vibration of the curvilinear stiffened plates were also taken into account by using of the von Karman's large deformation theory. The free vibration behavior of functionally graded plates considering in-plane material inhomogeneity was studied by Xue *et al.* [8] by using a NURBS-based IGA formulation based on a refined plate theory. The analysis of skew and elliptical plates were reported while the effects of geometry, boundary condition and material inhomogeneity were studied on the dynamic characteristics of the plate.

The conventional composite laminates are composed of a number of plies with unchanged directional mechanical properties throughout the whole geometry. This is achieved by using of either unidirectional (prepreg) or woven fiber reinforcements. The laminate then could be produced either with simple hand layup or a more complicated layup machines. If the fiber orientation or other fiber placement properties could be changed, the locally variable mechanical properties could be gained. With the automated fiber placement technology [9], it is possible to fabricate composite plies with variable fiber orientations within their geometrical domain. As a

result of changed fiber orientation (curvilinear fibers), the ply gains variable stiffness through the laminate geometry that is called as variable stiffness composite laminate.

Hyer *et al.*[10] and Gurdal and Olmedo [11, 12] reported their very first studies on curvilinear fiber VSCL plates. Akhavan and Ribeiro[13] investigated the free vibration of curvilinear fibers VSCL plates based on the third-order shear deformation theory (TSDT). A new p-version finite element formulation was developed to find the natural vibration modes. The changes in the laminate natural frequencies with the variation of the tow-orientation fiber angles were discussed. It was noted that the curvilinear fiber reinforcements could provide a higher flexibility in adjusting frequencies and mode shapes in comparison with the conventional straight fiber ones. Honda and Narita[14, 15] studied the natural frequencies of VSCL plates based on the classical plate theory. The significant effect of the curvilinear fiber reinforcements on the natural mode shapes and frequencies was shown. Fazilati[16] utilized enhanced spline-FSM to investigate the stability analysis of VSCL plates with delamination, adopting both the classical thin plate theory and the Reddy type higher order shear deformation theory. He [17] also utilized enhanced spline-FSM to investigate the supersonic linear flutter of rectangular VSCL panels containing square delamination zone.

Skew plates are widely used in many modern structural applications such as aircraft wings and marine vehicles. A useful and extensive survey has been provided by Liew and Wang [18] on the vibration of isotropic and orthotropic skew plates. Kapania and Singhvi [19] investigated free vibration analysis of generally laminated tapered skew plates used Rayleigh–Ritz method. Chebyshev’s polynomials were utilized as trial functions in order to express three displacement components on a given point. The boundary constraints are exerted by using number of appropriate springs with large stiffness’s at edges. Results were extracted for cases of isotropic, especially orthotropic, symmetric and asymmetric flat laminates. The free vibration of symmetrically laminated clamped skew plate was studied by Hosokawa *et al* [20]. The Green’s function approach was implemented and the effects of the plate skewness and fiber orientation angles on its natural frequencies and mode shapes were discussed. Wang *et al.*[21] investigated the free vibration of skew sandwich plates assuming an orthotropic core and laminated facings by using a p-Ritz method. The effects of variation of aspect ratios, boundary conditions, layup of facings, core and facings material on the vibration behavior was investigated. Malekzadeh [22] analyzed the natural frequencies of laminated composite thin skew plates by using a differential quadrature (DQ) approach based on classical plate theory. Green's strain in conjunction with von Karman assumptions were implemented in order to take in to account the geometrical nonlinearity effects. Houmat [23] proposed a p-element and studied the nonlinear free vibration of variable stiffness symmetric skew laminates based on thin plate theory and Von Karman strains. Assuming different fiber layup configurations, the effects of skewness on the frequency, normal mode, and degree of hardening have been studied.

According to the aforementioned literature reviews, while many researches are reported on the mechanical behavior of VSCL panels, to the best of the authors’ knowledge, the free vibration analysis of VSCL skew panels is not completely addressed. Therefore, in the present paper, a NURBS based isogeometric formulation is developed to investigate the free vibration analysis of composite laminated skew plate subjected to various sets of boundary conditions. Variable stiffness properties due to curvilinear fiber orientation in the laminate plies is assumed. An enhanced isogeometric formulation is developed based on the classical plate theory (CLT). The

NURBS basis functions of cubic order are employed in order to build the plate's geometry while simultaneously serve as the shape functions for solution field approximation in finite element analysis. To show the effectiveness and accuracy of the developed CLT IGA formulation, typical free vibration problems are conducted and the extracted results are compared to referenced ones. The effects of curvilinear fiber angles, different geometries and various end constraints are evaluated on the VSCL skew panel behavior.

2. Isogeometric functions

Defining the NURBS basis functions and their directional derivatives are fundamentals of IGA formulation development. The NURBS function is a generalization of B-spline curve. A B-spline one dimensional curve could be defined over parametric space $[0,1]$ by using of a set of non-decreasing numbers called knot vector $\Xi(\zeta) = \{\zeta_1=0, \dots, \zeta_i, \dots, \zeta_{n+p+1}=1\}^T$ ($\zeta_i \leq \zeta_{i+1}$), together with a set of control points P_i ($i=1, \dots, n$). n and p are the number of spline basis functions and the order of spline basis functions, respectively. The non-zeros knot span $[\zeta_i \leq \zeta_{i+1})$, behaviors as an element in isogeometric methodology. A knot vector $\Xi(\zeta)$ may called an open knot vector if the two end knots are repeated $p+1$ times.

With a given knot vector $\Xi(\zeta)$, the B-spline basis function, written as $N_{i,p}(\zeta)$, is defined recursively as follows[24]:

$$N_{i,0}(\zeta) = \begin{cases} 1 & \text{if } \zeta_i \leq \zeta < \zeta_{i+1} \\ 0 & \text{otherwise} \end{cases} \quad \text{for } p = 0 \quad (1)$$

$$N_{i,p}(\zeta) = \frac{\zeta - \zeta_i}{\zeta_{i+p} - \zeta_i} N_{i,p-1}(\zeta) + \frac{\zeta_{i+p+1} - \zeta}{\zeta_{i+p+1} - \zeta_{i+1}} N_{i+1,p-1}(\zeta) \quad \text{for } p \geq 1 \quad (2)$$

The one dimensional NURBS basis function, $R_{i,p}(\zeta)$, is constructed using weighted average of some B-spline basis functions [24] as,

$$R_{i,p}(\zeta) = \frac{N_{i,p}(\zeta)w_i}{\sum_{j=1}^n N_{j,p}(\zeta)w_j} \quad (3)$$

where w_i is the i^{th} weight coefficient; the NURBS basis function is degenerated into a B-spline basis function for $w_i = 1$.

In a similar manner, the bivariate NURBS basis function (for case of NURBS surface) is defines as

$$R_{i,j}^{p,q}(\zeta, \eta) = \frac{N_{i,p}(\zeta)N_{j,q}(\eta)w_{i,j}}{\sum_{i=1}^n \sum_{j=1}^m N_{i,p}(\zeta)N_{j,q}(\eta)w_{i,j}} = \frac{N_{i,p}(\zeta)N_{j,q}(\eta)w_{i,j}}{W(\zeta, \eta)} \quad (4)$$

where $w_{i,j}$ represents the 2D weight coefficients; $N_{j,q}(\eta)$ is the B-spline basis of order q defined on the knot vector $\Xi(\eta)$, followed by the recursive formula shown in equations (1) and (2). The NURBS basis functions has the same properties as B-splines. By using the NURBS basis functions, a NURBS surface of order p in the ζ direction and order q in the η direction may be constructed as follows:

$$S(\zeta, \eta) = \sum_{i=1}^n \sum_{j=1}^m R_{i,j}^{p,q}(\zeta, \eta) P_{i,j} \tag{5}$$

where $P_{i,j}$ represents the coordinates of control points in two dimensions. The first derivatives of the NURBS basis function $R_{i,j}^{p,q}(\zeta, \eta)$ with respect to each parametric variable are derived by applying the quotient rule to the equation (4) as

$$\frac{\partial R_{i,j}^{p,q}(\zeta, \eta)}{\partial \zeta} = w_{i,j} \frac{\frac{\partial N_{i,p}(\zeta)}{\partial \zeta} N_{j,q}(\eta) W(\zeta, \eta) - \frac{\partial W(\zeta, \eta)}{\partial \zeta} N_{i,p}(\zeta) N_{j,q}(\eta)}{(W(\zeta, \eta))^2} \tag{6a}$$

$$\frac{\partial R_{i,j}^{p,q}(\zeta, \eta)}{\partial \eta} = w_{i,j} \frac{\frac{\partial N_{j,q}(\eta)}{\partial \eta} N_{i,p}(\zeta) W(\zeta, \eta) - \frac{\partial W(\zeta, \eta)}{\partial \eta} N_{i,p}(\zeta) N_{j,q}(\eta)}{(W(\zeta, \eta))^2} \tag{6b}$$

The first derivatives of the weighting function, $W(\zeta, \eta)$, with respect to each parametric variable are given by

$$\frac{\partial W(\zeta, \eta)}{\partial \zeta} = \sum_{i=1}^n \sum_{j=1}^m \frac{\partial N_{i,p}(\zeta)}{\partial \zeta} N_{j,q}(\eta) w_{i,j} \tag{7a}$$

$$\frac{\partial W(\zeta, \eta)}{\partial \eta} = \sum_{i=1}^n \sum_{j=1}^m \frac{\partial N_{j,q}(\eta)}{\partial \eta} N_{i,p}(\zeta) w_{i,j} \tag{7b}$$

Higher-order derivatives of the NURBS basis function and the weighting function can be obtained via a similar process.

3. Governing equations and discretization

A typical symmetric laminated skew plate with length a , width b , and a Cartesian coordinate system is assumed with x and y rectangular coordinate axes located on the mid-plane of the undeformed laminated plate. (u, v, w) are displacements of the plate in the (x, y, z) direction (Figure 1). Based on the classical laminate plate theory, the displacement field of the plate is:

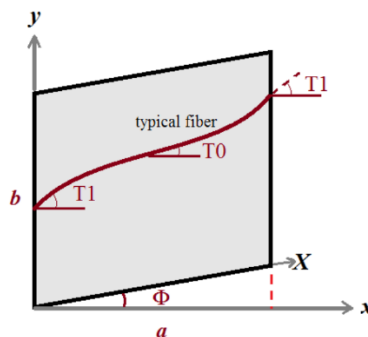


Fig 1. Reference fiber path in typical VSCL skew plate with curvilinear fibres.

$$u = \{u \ v \ w\}^T = \left\{ -z \frac{\partial}{\partial x} \quad -z \frac{\partial}{\partial y} \quad 1 \right\}^T w = Tw \tag{8}$$

It is to be notified that in-plane displacements are overlooked and therefore the assumed approximating displacement field are limited to the case of bending and twisting behavior of laminated plate. In this study, the NURBS basis function is employed for both the parameterization of the geometry and the approximation of the deflection field $w(x)$ as follows,

$$w^h(x(\zeta)) = \sum_{I=1}^{n \times m} \phi_I(\zeta) w_I \tag{9}$$

$$x(\zeta) = \sum_{I=1}^{n \times m} \phi_I(\zeta) \tilde{x}_I \tag{10}$$

in the above equations, $\zeta = (\zeta, \eta)$ are parametric coordinate sets, $x = (x, y)$ are physical coordinate sets, X_I denotes a control mesh consisting of $n \times m$ control points, w_I signify the displacement field at each control point (i.e control variables), $\phi_I(\zeta)$ are the bivariate NURBS basis functions of order p and q along ζ and η directions, respectively. The strains and stresses sets on the geometry are given as [6],

$$\varepsilon_p = \left\{ -\frac{\partial^2}{\partial x^2} \quad -\frac{\partial^2}{\partial y^2} \quad -2\frac{\partial^2}{\partial x \partial y} \right\}^T w = Lw \tag{11}$$

$$\sigma_p = \{M_x \ M_y \ M_{xy}\}^T \tag{12}$$

M_x , M_y and M_{xy} are moments corresponding to the bending and twisting. The relationship between strains and stresses could be expressed as,

$$\sigma_p = D\varepsilon_p \tag{13}$$

where D is the bending stiffness and is given as follows:

$$D_{ij} = \int_{-\frac{h}{2}}^{\frac{h}{2}} \bar{Q}_{ij}(x)(1, z, z^2) dz \tag{14}$$

and $\bar{Q}_{ij}(x)$ are the elements of anisotropic material constant matrix and defined by

$$\begin{aligned} \bar{Q}_{11}(x) &= Q_{11} \cos^4 \theta(x) + 2(Q_{12} + 2Q_{66}) \sin^2 \theta(x) \cos^2 \theta(x) + Q_{22} \sin^4 \theta(x), \\ \bar{Q}_{12}(x) &= (Q_{11} + Q_{22} - 4Q_{66}) \sin^2 \theta(x) \cos^2 \theta(x) + Q_{12} (\sin^4 \theta(x) + \cos^4 \theta(x)), \\ \bar{Q}_{22}(x) &= Q_{11} \sin^4 \theta(x) + 2(Q_{12} + 2Q_{66}) \sin^2 \theta(x) \cos^2 \theta(x) + Q_{22} \cos^4 \theta(x), \\ \bar{Q}_{16}(x) &= (Q_{11} - Q_{12} - 2Q_{66}) \sin \theta(x) \cos^3 \theta(x) - (Q_{22} - Q_{12} - 2Q_{66}) \sin^3 \theta(x) \cos \theta(x), \\ \bar{Q}_{26}(x) &= (Q_{11} - Q_{12} - 2Q_{66}) \sin^3 \theta(x) \cos \theta(x) - (Q_{22} - Q_{12} - 2Q_{66}) \sin \theta(x) \cos^3 \theta(x), \\ \bar{Q}_{66}(x) &= (Q_{11} + Q_{22} - 2Q_{12} - 2Q_{66}) \sin^2 \theta(x) \cos^2 \theta(x) + Q_{66} (\sin^4 \theta(x) + \cos^4 \theta(x)). \end{aligned} \tag{15}$$

With

$$Q_{11} = \frac{E_1}{1 - \nu_{12}\nu_{21}}, Q_{22} = \frac{E_2}{1 - \nu_{12}\nu_{21}}, Q_{12} = \nu_{12}Q_{22} = \nu_{21}Q_{11}, Q_{66} = G_{12} \tag{16}$$

In the above equations E_1 and E_2 are the Young's moduli parallel to and perpendicular to the fiber local direction, G_{12} is the shear modulus, ν_{12} and ν_{21} are the Poisson's ratios and $\Theta(x)$ is the fiber orientation angle with respect to and along the x -axis of the plate. As suggested by Gürdal and Olmedo [11], the orientation of the reference fiber path in layer k of the VSCL plate is given by

$$\theta^k(x) = \frac{2(T_1^k - T_0^k)}{a}|x| + T_0^k \tag{17}$$

where T_0^k and T_1^k gives the angle between the fiber and the x -axis at the plate center ($x = 0$), and at the plate ends ($x = \pm a/2$), respectively. The fiber path that corresponds to equation (17) is represented by $\langle T_0^k, T_1^k \rangle$ where $T_0^k = T_1^k$ may represents a straight fiber case.

Based on an energy approach, the governing equations of the free vibration problem of the composite laminated plate could be expressed as [6]:

$$\frac{d}{dt} \frac{1}{2} \int_{\Omega} \rho \frac{\partial}{\partial w} [(Tw)^T (Tw)] d\Omega + \frac{1}{2} \int_{\Omega} \frac{\partial}{\partial w} [(Lw)^T D(Lw)] d\Omega = 0 \tag{18}$$

Here ρ and Ω are mass density of the constructing material and the geometry total volume, respectively. By substituting the deflection function, w , from equation (9) into equation (18), and applying some further manipulations, an eigenvalue governing equation of the free vibration could be obtained as,

$$(K - \omega^2 M)Q = 0 \tag{19}$$

ω is the structural natural frequency, Q is the eigenvector of the form $\{w_1, w_2, \dots, w_{ncp}\}$ including the deflections of all control points in the geometry domain, and M and K are called the global mass and stiffness matrices where are given by

$$K_{ij} = \int_{\Omega} B_i^T D B_j d\Omega \tag{20}$$

$$M_{ij} = \int_{\Omega} \rho \tilde{B}_i^T \tilde{B}_j d\Omega \tag{21}$$

$$B_i = \left\{ -\phi_{i,xx} \quad -\phi_{i,yy} \quad -2\phi_{i,xy} \right\} \tag{22}$$

$$\tilde{B}_i = \left\{ -z\phi_{i,x} \quad -z\phi_{i,y} \quad \phi_i \right\} \tag{23}$$

4. Results and discussion

For all calculation case studies presented in the remainder of the present paper, the cubic order NURBS basis functions and a 15x15 NURBS elements (18x18 control points) are employed and a 4x4 Gauss quadrature is utilized in numerical integration over each element. Different boundary conditions including simply supported (S), clamped (C), and free (F) are also considered. The clamped boundary conditions could be applied through limiting the rotations by imposing constraint on two adjacent rows of control points on the boundary [5]. The following material properties and geometrical parameters of laminated plates are used [13]:

$$E_1 = 173Gpa, E_2 = 7.2Gpa, G_{12} = 3.76Gpa, \nu_{12} = 0.29$$

$$\rho = 1540kg / m^3, a = b = 1m, h = 0.01m \tag{24}$$

Some representative comparisons are made to show the accuracy and effectiveness of the present formulation.

The first five natural frequencies of fully simply supported (SSSS) three-ply curvilinear square panel with variable fiber angle layup [$\langle 30,0 \rangle, \langle 45,90 \rangle, \langle 30,0 \rangle$] is investigated. For models with the similar degrees of freedom (dof), the problem of free vibration is solved using the CLT Rayleigh-Ritz method (RRM). The results of CLT IGA, CLT RRM besides the prediction of the enhanced p-version higher order (HLT) FEM of Akhavan and Ribeiro [13] are presented in Table 1. The results signify the fast convergency of the IGA formulation in comparison with RRM. The results also authenticate the good accuracy of the IGA calculation with respect to HLT pFEM results despite using lower plate theory assumptions.

Table 1. Natural frequencies (Hz) of SSSS VSCL square plate [$\langle 30,0 \rangle, \langle 45,90 \rangle, \langle 30,0 \rangle$]

Model dof	Method	Natural frequency (Hz)		
		1	2	3
100	RRM [25]	310.046	506.183	849.467
	CLT IGA	309.602	505.302	851.873
400	RRM [25]	309.673	505.505	848.655
	CLT IGA	309.332	504.787	847.791
900	RRM [25]	309.563	505.306	848.459
	CLT IGA	309.319	504.785	847.744
1600	RRM [25]	309.508	505.207	848.368
	CLT IGA	309.314	504.786	847.742
2025	RRM [25]	309.487	505.178	848.338
	CLT IGA	309.315	504.791	847.748
-	HLT pFEM [13]	308.799	503.799	845.509

The first six natural frequencies of a three-layer square VSCL plate, under fully free (FFFF), simply supported (SSSS), and clamped (CCCC) edge constraints is investigated. The variable fiber angle layup of [$\langle 0,45 \rangle, \langle -45,-60 \rangle, \langle 0,45 \rangle$] is assumed. According to Table 2, the present results have good satisfactory agreement with p-version HLT FEM results calculated by Akhavan and Ribeiro [13].

The first eight natural frequencies are calculated in case of fully simply supported (SSSS) and fully clamped (CCCC) laminated skew plates of layup $[(45/-45)_2/45]$. The geometrical parameters of $a = b = 1, a/h = 100$, with skew angles $\Phi = 0, 30, 45$ are considered. According to the presented results in Table 3, the IGA calculations are in satisfactory agreement with classical plate theory Rayleigh–Ritz method predictions of Wang [26].

Table 2. Natural frequencies (Hz) of VSCL plate [$\langle 0,45 \rangle, \langle -45, -60 \rangle, \langle 0,45 \rangle$]

Mode	FFFF		SSSS			CCCC		
	HLT pFEM [13]	CLT IGA	HLT [13]	pFEM	CLT IGA	HLT [13]	pFEM	CLT IGA
1	140.946	141.282	358.488		358.431	579.398		582.189
2	170.210	170.319	589.900		590.576	821.532		826.232
3	344.570	345.607	960.361		962.924	1225.79		1233.797
4	477.563	478.834	1075.21		1081.577	1493.76		1515.583
5	592.531	594.585	1327.88		1334.155	1726.96		1754.643
6	715.990	719.894	1474.67		1471.940	1775.16		1789.947

Table 3. Fundamental natural frequency parameters of fully simply supported and clamped laminated skew panels [$\langle 45/-45 \rangle_2/45$] ($\Omega = \omega a^2 / \pi^2 h \sqrt{\rho/E_2}$)

B.Cs	Φ	Method	frequency parameter Ω							
			1	2	3	4	5	6	7	8
SSSS	0	IGA	2.4337	4.9855	6.1806	8.4841	10.2497	11.6422	12.8194	15.2089
		RRM [26]	2.4339	4.9865	6.1818	8.4870	10.2536	11.6464	12.8260	15.2173
	30	IGA	2.6115	5.6889	6.8295	9.4740	11.8836	13.2284	14.2738	17.3268
		RRM [26]	2.6119	5.6902	6.8316	9.4773	11.8900	13.2355	14.2809	17.3382
	45	IGA	3.3164	6.8981	9.6835	10.7160	15.5244	16.1343	19.3271	21.2834
		RRM [26]	3.3182	6.9002	9.6908	10.7206	15.5318	16.1447	19.3481	21.3005
CCCC	0	IGA	3.9006	7.1451	8.4574	11.2081	13.3175	14.7396	16.1205	18.8062
		RRM [26]	3.9009	7.1464	8.4585	11.2112	13.3216	14.7425	16.1271	18.8145
	30	IGA	4.5426	8.3801	9.8783	12.8492	15.6839	17.4798	18.3314	21.9224
		RRM [26]	4.5431	8.3819	9.8810	12.8533	15.6906	17.4889	18.3396	21.9364
	45	IGA	6.3037	10.8165	14.4884	15.4646	21.052	22.0584	25.8634	27.6336
		RRM [26]	6.3048	10.8193	14.4949	15.4692	21.062	22.0759	25.8849	27.6869

The fundamental natural frequency parameter ($\Omega = \omega a \sqrt{\rho/E_2}$) are extracted in case of fully clamped (CCCC) variable stiffness skew plates of 3, 5, and 8 variable stiffness layers. Three variable fiber orientation layups of I: [$\langle +T_0, T_1 \rangle, \langle -T_0, T_1 \rangle, \langle +T_0, T_1 \rangle$], II: [$\langle +T_0, T_1 \rangle, \langle -T_0, T_1 \rangle, \langle +T_0, T_1 \rangle$]₂ and III: [$\langle +T_0, T_1 \rangle, \langle -T_0, T_1 \rangle$]₂_S are taken into account. The geometric parameters are $a = b = 0.5$ m, $h = 0.005$ m, and $\Phi = 30, 45$. The fiber placement parameters are $T_0 = 45$ and $T_1 = 40, 65, 90$. The middle plate fiber orientation (T_0) is kept unchanged while the fiber orientations at the panel

longitudinal ends (T_1) are altered. According to Table 4, the CLT IGA results are in satisfactory agreement with CLT FEM predictions presented by Houmat [23]. The IGA method provides more conservative frequencies (lower ones) in case of layups I and II. The layups with lower T_1 exhibits the best design with higher frequencies. It also could be notifying that the layup I shows more sensitivity to the panel skewness.

Table 4. Natural frequencies (Hz) of 3, 5 and 8-layer symmetric VSCL skew plate

	$(T_0=45)$	$\Phi=30$		$\Phi=45$		
		T_1	FEM [23]	IGA	FEM [23]	IGA
layup I	40		0.4496	0.4477	0.6913	0.6837
	65		0.3337	0.4325	0.6344	0.6316
	90		0.4128	0.4126	0.5677	0.5667
layup II	40		0.4517	0.4511	0.6694	0.6668
	65		0.4214	0.4210	0.6014	0.5998
	90		0.3951	0.3951	0.5343	0.5340
layup III	40		0.4447	0.4448	0.6484	0.6491
	65		0.4093	0.4093	0.5762	0.5764
	90		0.3820	0.3821	0.5116	0.5116

The natural frequency parameters ($\Omega = \omega a^2 \sqrt{\rho h / D}$) are calculated in case of cantilevered (CFFF) skew laminate of layup $[(\Theta / - \Theta)_2 / \Theta]$. The geometrical parameters of $a = b = 1$, $a/h = 100$, and $\Phi = 0, 60$ are considered. According to Table 5, the IGA calculations are in good agreement with CLT Rayleigh–Ritz predictions presented by Han and Dickinson [27]. The results show the effectiveness of the developed formulation in analyzing versatile boundary constraint sets.

Table 5. Dimension-less natural frequencies of CFFF laminated skew panel $[(\Theta / - \Theta)_2 / \Theta]$

Θ	Φ	Method	Mode				
			1	2	3	4	5
0	0	IGA	3.511567	4.734656	9.106148	18.3375	22.00242
		RRM [27]	3.5143	4.7373	9.1101	18.347	22.021
	60	IGA	4.231318	7.905243	18.51047	26.91552	34.36292
		RRM [27]	4.2328	7.8953	18.521	26.911	34.401
30	0	IGA	2.544406	5.948861	12.62251	16.41291	21.5345
		RRM [27]	2.5443	5.9493	12.634	16.416	21.539
	60	IGA	3.243181	9.252418	20.1666	27.31974	40.2716
		RRM [27]	3.2417	9.2568	20.139	27.293	40.281

The natural frequencies are calculated for CCCC, SSSS and FFFF symmetric three-layer VSCL plate. Two variable fiber orientation 3-layer layups of *I*: [$\langle 30,0 \rangle, \langle 45,90 \rangle, \langle 30,0 \rangle$] and *II*: [$\langle 90,45 \rangle, \langle 60,30 \rangle, \langle 90,45 \rangle$] are considered. The results for the first five natural frequencies for three skewness angle values, $\Phi=0, 15$ and 30 are presented in Table 6. According to the results, the layup design *I* for three skewness angle values is a more efficient design with 6 to 10 percent higher frequencies dependent to the boundary conditions. It also indicates the significance of the boundary constraints on the frequencies where a clamped constraint could boost the fundamental frequency by a factor of 2 with regard to simply supported one. It also shows that with increase in the skew angle, a decreasing-increasing manner in case of layup *I* exists while a fully decreasing behavior could be observed in case of layup *II*.

Table 6. Natural frequencies (Hz) for all BCs three-ply VSCL Skew ($\Phi=0$) plate

layu p	Mode	CCCC			SSSS			FFFF		
		$\Phi=0$	$\Phi=15$	$\Phi=30$	$\Phi=0$	$\Phi=15$	$\Phi=30$	$\Phi=0$	$\Phi=15$	$\Phi=30$
I	1	665.46	656.58	664.35	309.33	296.95	313.34	110.48	116.56	97.77
	2	863.71	827.74	861.57	504.78	467.94	514.03	177.32	176.02	204.70
	3	1239.92	1179.11	1236.95	847.81	808.56	855.48	266.62	304.08	254.78
	4	1714.44	1709.99	1708.83	1139.50	1135.65	1145.70	459.92	482.39	482.13
	5	1790.21	1745.67	1783.55	1283.51	1261.71	1289.86	469.20	551.14	520.84
II	1	710.00	671.45	647.46	329.68	316.46	310.97	123.11	137.80	128.16
	2	914.58	887.19	875.01	538.35	529.91	530.91	151.31	151.53	177.67
	3	1340.50	1360.82	1388.29	884.32	917.67	967.24	277.92	336.83	386.74
	4	1703.47	1609.32	1525.41	1092.88	1029.30	976.95	389.80	396.16	394.79
	5	1857.71	1710.38	1607.81	1277.74	1179.70	1102.56	404.74	406.36	403.01

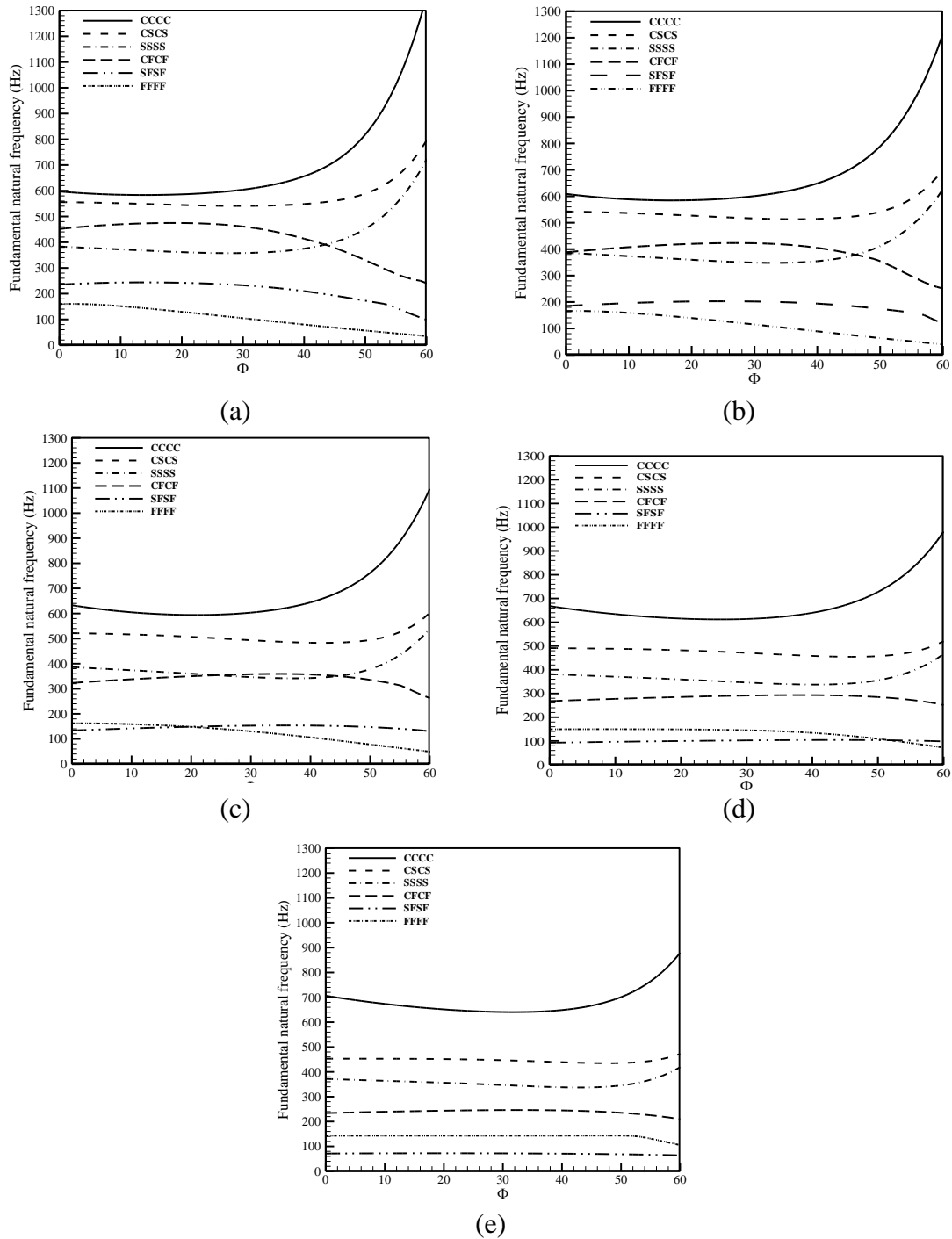


Fig 2. Fundamental natural frequency for skew plate under skewness angle values a) $T_0=15$, b) $T_0=30$, c) $T_0=45$, d) $T_0=60$, e) $T_0=75$.

A symmetric variable fiber-orientation panel is considered with six different boundary condition sets, namely CCCC, CSCS, SSSS, CFCF, SFSF and FFFF. The variations of fundamental natural frequency with skewness angle (Φ) as well as boundary condition set for five lay-up $[\pm<15,45>]_s$,

, $[\pm<30,45>]_s$, $[\pm<45,45>]_s$, $[\pm<60,45>]_s$ and $[\pm<75,45>]_s$ are extracted and depicted in Figures 2(a) to 2(e), respectively. According to the presented results, the fundamental natural frequency in case of CCCC, CCSS and SSSS boundary condition sets grows with skewness angle. For cases with at least one free edge, the fundamental frequency is higher for smaller skew angles. According to Figure 2(a) the SFSF plate shows higher frequencies than FFFF curve for $[\pm<15,45>]_s$. As T_0 increases, the difference of the two curves reduces (see Figure 2(b)). With increasing of T_0 fiber angle, according to Figure 2(c), the FFFF frequencies dominates the SFSF ones for skew angles between $\Phi=0$ and $\Phi=20$. For $T_0=60$, Figure 2(d) shows higher frequencies for FFFF than SFSF in the skew interval of $\Phi=0$ to $\Phi=55$. This dominance could be observed in more extended skew angle interval for $T_0=75$ as in Figure 2(e).

Symmetric four-layer rectangular VSCL plate whit layup $[\pm<T_0,45>]_s$ is considered where the middle-length fiber angle (T_0) is varied from 0 to 90 degrees. Fundamental natural frequency for skew plate ($\Phi=45$) for six different boundary condition sets is calculated and depicted in Figure 3. According to the results, the fundamental natural frequency for boundary conditions CCCC, SSSS and CSCS with increase the middle-length fiber angle (T_0), initially decreases and then increases as the skew angle raises. For boundary condition sets with two opposite edges free, the fundamental natural frequency follows an increasing-decreasing route. Also, the fundamental natural frequency for FFFF boundary condition advances the SFSF for T_0 angles higher than 55 degrees.

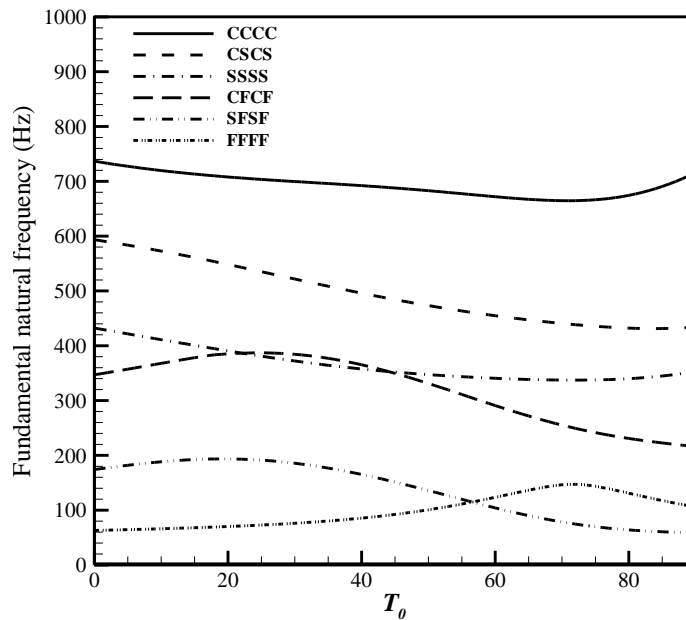


Fig 3. Fundamental natural frequency for skew plate under T_0 ($\Phi=45$).

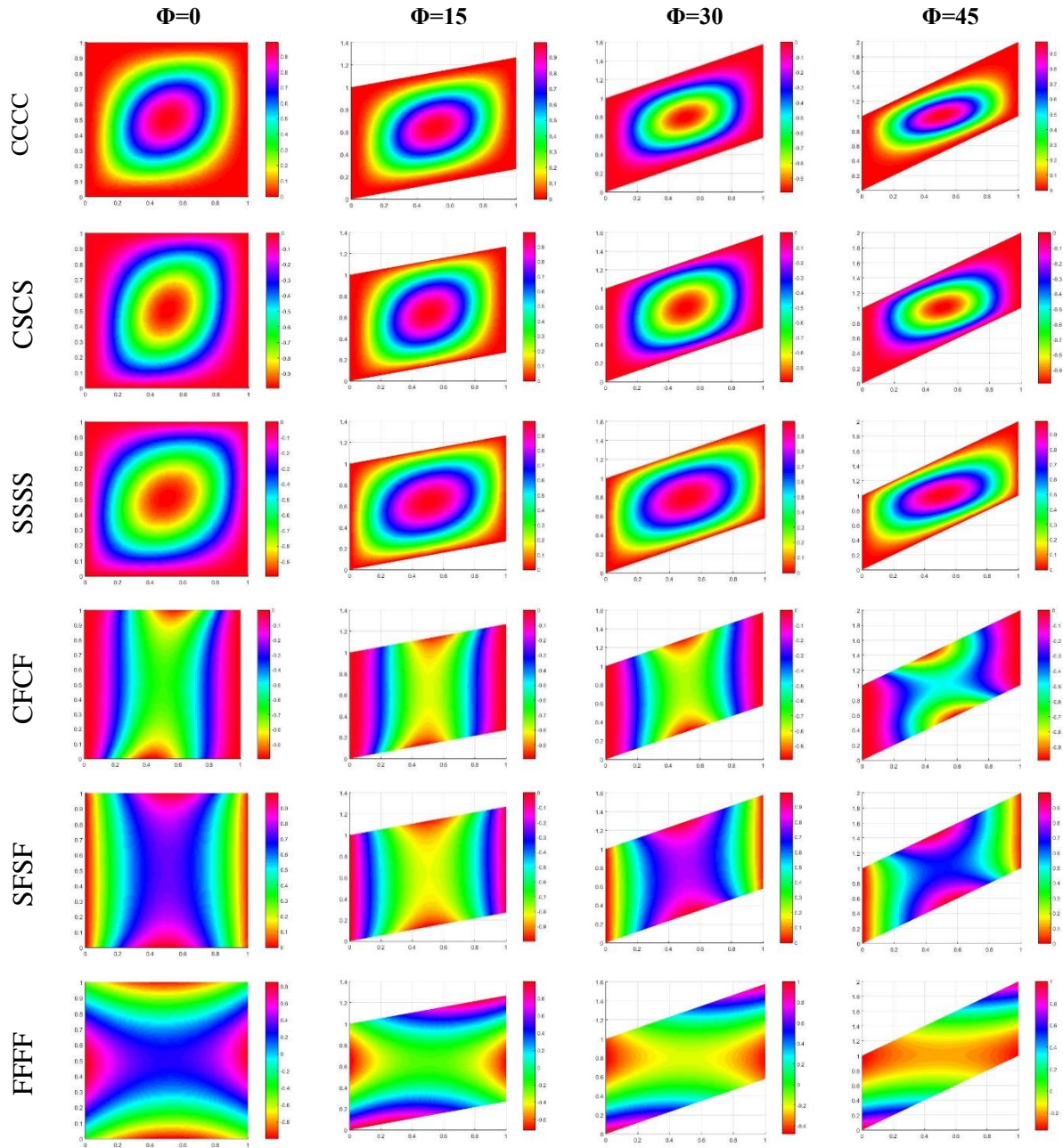
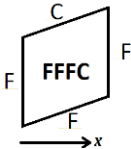
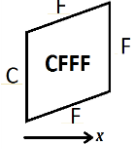
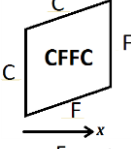
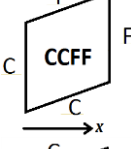
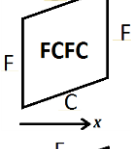
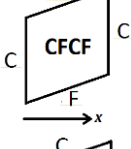
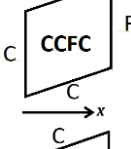
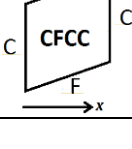


Fig 4. Fundamental mode shapes of VSCL Skew plate with layup $[\pm<30,45>]_s$

The fundamental natural mode shapes of CCCC, CSCS, SSSS, CFCF, SFSF and FFFF symmetric four-layer skew plate $[+<30,45>]_s$ for four skewness angle values, (i.e. $\Phi=0$, $\Phi=15$, $\Phi=30$, and $\Phi=45$) are depicted in Figure 4.

Table 6. Fundamental natural frequencies (Hz) of four-layer VSCL skew plate ($\Phi=10$) with different boundary constraint sets

boundary constraint	Layup	
	$[\pm<30,45>]_s$	$[\pm<60,45>]_s$
	34.6961	55.6987
	59.2507	40.0253
	106.7196	109.8459
	121.9922	130.1349
	235.0657	360.0266
	409.1717	278.5512
	300.2391	396.6129
	439.0274	337.6396

In order to study the effects of different end constraints on the dynamic characteristics of the VSCL skew plates, a laminated four-layer skew panel subjected to clamped and free constraints on its edges is considered. Two layups with similar $T1=45$ and different $T0$ of 30 and 60 degrees are taken into account. The IGA results are given in Table 6. According to the results, the behavior of the panel and its sensitivity to the end constraint is a function of middle length fiber orientation. The results imply that in case of $T0=60$, the panels with more clamped constraints on

the inclined side edges show higher dynamic stability (higher natural frequencies) while in the layup with $T_0=30$, an opposite rule could be observed. In other words, the $[\pm\langle 60,45 \rangle]$ s skew panel with boundary condition sets of FCFC, FFFC and CCFC offer higher panel frequencies than CFCF, CFFF and CFCC sets, respectively. For the case of adjacent double clamped edges (CCFF and CFFC), the two layups have the same behavior such that acute angle between the clamped edges defines the more stable panel. The layup with $T_0=30$, is observed to be more sensitive to the variation of the clamped edge position as more changes in the fundamental natural frequency could be occurred. The best dynamic characteristics could be found for CFCC and FCFC end constraint sets in cases of 30 and 60 degrees T_0 , respectively.

5. Conclusions

An enhanced isogeometric analysis formulation based on classical plate theory is developed and applied to the problem of free vibration of variable stiffness composite laminated skew plates. The cubic NURBS basis functions are employed in order to approximate the geometry while simultaneously serving as the shape functions for solution field approximation in the analysis. The laminate's plies stiffness is assumed to vary linearly throughout the geometry due to angle variation of fiber reinforcements. The representative results showed the good accuracy and effectiveness of the formulation in the handling of free vibration problem of VSCL skew panels with versatile end constraints. The effects of variable fiber-orientation, lay-up, boundary conditions and the panel skew angle on the dynamic characteristics are addressed. According to the presented calculations, the following hint may be declared:

- It is found that the convergence rate of the IGA calculations are higher than that of RRM.
- Clamped constraint could boost the fundamental frequency by a factor of 2 with regard to simply supported one.
- Higher skew angles increase the fundamental natural frequency under CCCC, CCSS and SSSS boundary conditions while reduce fundamental natural frequency in boundary condition sets with at least one free edge.
- For boundary condition sets with two opposite edges free, when T_0 increased, the fundamental natural frequency follows an increasing-decreasing route.
- The skew panel with layup I is highly sensitive to the skewness angle.
- The layups with lower T_1 fiber angle offer higher natural frequencies.
- The dynamic behavior of the VSCL skew panels while the end constraints are varying are dependent on T_0 .
- Adjacent double clamped edges with amongst acute angle provide a more stable panel.

References

- [1] T.J.R. Hughes, J.A. Cottrell, Y. Bazilevs, Isogeometric analysis: CAD, finite elements, NURBS, exact geometry and mesh refinement, *Computer methods in applied mechanics and engineering*, 194 (2005) 4135-4195.
- [2] Y. Bazilevs, V.M. Calo, T.J.R. Hughes, Y. Zhang, Isogeometric fluid-structure interaction: theory, algorithms, and computations, *Computational mechanics*, 43 (2008) 3-37.
- [3] F. Auricchio, L.B. Da Veiga, C. Lovadina, A. Reali, The importance of the exact satisfaction of the incompressibility constraint in nonlinear elasticity: mixed FEMs versus NURBS-based approximations, *Computer Methods in Applied Mechanics and Engineering*, 199 (2010) 314-323.
- [4] J.A. Cottrell, T.J.R. Hughes, A. Reali, Studies of refinement and continuity in isogeometric structural analysis, *Computer methods in applied mechanics and engineering*, 196 (2007) 4160-4183.
- [5] S. Shojaee, N. Valizadeh, E. Izadpanah, J. Kiendl, Free vibration and buckling analysis of laminated composite plates using the NURBS-based isogeometric approach, *Finite Elements Analysis Design*, 61 (2012) 23-34.
- [6] S. Shojaee, N. Valizadeh, E. Izadpanah, T. Bui, T.-V. Vu, Free vibration and buckling analysis of laminated composite plates using the NURBS-based isogeometric finite element method, *Composite Structures*, 94 (2012) 1677-1693.
- [7] X.C. Qin, C.Y. Dong, F. Wang, X.Y. Qu, Static and dynamic analyses of isogeometric curvilinearly stiffened plates, *Applied Mathematical Modelling*, 45 (2017) 336-364.
- [8] Y. Xue, G. Jin, H.u. Ding, M. Chen, Free vibration analysis of in-plane functionally graded plates using a refined plate theory and isogeometric approach, *Composite Structures*, 192 (2018) 193-205.
- [9] K. Kozaczuk, Automated fiber placement systems overview, *Prace Instytutu Lotnictwa*, 4 (2016) 52-59.
- [10] M.W. Hyer, R.F. Charette, Use of curvilinear fiber format in composite structure design, *AIAA journal*, 29 (1991) 1011-1015.
- [11] Z. Gurdal, R. Olmedo, In-plane response of laminates with spatially varying fiber orientations-variable stiffness concept, *AIAA journal*, 31 (1993) 751-758.
- [12] R. Olmedo, Z. Gurdal, Buckling response of laminates with spatially varying fiber orientations, in: *Proceedings of the 34th AIAA/ASME/ASCE/AHS/ASC Structures, Structural Dynamics and Materials (SDM) Conference*, La Jolla, CA 1993.
- [13] H. Akhavan, P. Ribeiro, Natural modes of vibration of variable stiffness composite laminates with curvilinear fibers, *Composite Structures*, 93 (2011) 3040-3047.
- [14] S. Honda, Y. Narita, Vibration design of laminated fibrous composite plates with local anisotropy induced by short fibers and curvilinear fibers, *Composite Structures*, 93 (2011) 902-910.
- [15] S. Honda, Y. Narita, Natural frequencies and vibration modes of laminated composite plates reinforced with arbitrary curvilinear fiber shape paths, *Journal of Sound and Vibration*, 331 (2012) 180-191.
- [16] J. Fazilati, Stability analysis of variable stiffness composite laminated plates with delamination using spline-FSM, *Latin American Journal of Solids and Structures*, 14 (2017) 528-543.
- [17] J. Fazilati, Panel flutter of curvilinear composite laminated plates in the presence of delamination, *Journal of Composite Materials*, (2018).
- [18] K.M. Liew, C.M. Wang, Vibration studies on skew plates: treatment of internal line supports, *Computers & structures*, 49 (1993) 941-951.
- [19] R.K. Kapania, S. Singhvi, Free vibration analyses of generally laminated tapered skew plates, *Composites Engineering*, 2 (1992) 197-212.
- [20] K. Hosokawa, Y. Terada, T. Sakata, Free vibrations of clamped symmetrically laminated skew plates, *Journal of sound and vibration*, 189 (1996) 525-533.
- [21] C.M. Wang, K.K. Ang, L. Yang, E. Watanabe, Free vibration of skew sandwich plates with laminated facings, *Journal of sound and vibration*, 235 (2000) 317-340.
- [22] P. Malekzadeh, A differential quadrature nonlinear free vibration analysis of laminated composite skew thin plates, *Thin-walled structures*, 45 (2007) 237-250.
- [23] A. Houmat, Nonlinear free vibration analysis of variable stiffness symmetric skew laminates, *European Journal of Mechanics-A/Solids*, 50 (2015) 70-75.
- [24] L. Piegl, W. Tiller, *The NURBS Book* in, Springer, Berlin Heidelberg, 1995.

- [25] V. Khalafi, J. Fazilati, Supersonic Flutter Analysis of Curvilinear Fiber Variable Stiffness Composite Laminated Plates, in: 5th International Conference on Composites: Characterization, Fabrication and Application, CCFA-5 2016.
- [26] S. Wang, Vibration of thin skew fibre reinforced composite laminates, *Journal of sound and vibration*, 201 (1997) 335-352.
- [27] W. Han, S.M. Dickinson, Free vibration of symmetrically laminated skew plates, *Journal of sound and vibration*, 208 (1997) 367-390.